

SYNTHESIS AND SPECTRAL ANALYSIS OF CHARGE-TRANSFER COMPLEXES OF TRIAMTERENE DRUG WITH 2,4,6-TRINITROPHENOL, 4-NITROPHENOL, 4-NITROACETOPHENONE, AND *m*-DINITROBENZENE ACCEPTORS IN THE SOLID-STATE FORM: EXPERIMENTAL AND DFT STUDIES**

Abeer A. El-Habeeb

Department of Chemistry, College of Science at Princess Nourah bint Abdulrahman University, Riyadh 11671, Saudi Arabia; e-mail: dr_abeer_2@hotmail.com

*The present work aims to focus on the synthesis and spectral studies of the charge-transfer interaction between the nitro organic acceptors molecules [e.g., 2,4,6-trinitrophenol (PA), 4-nitrophenol (4-NP), 4-nitroacetophenone (4-NAP), and *m*-dinitrobenzene (*m*-DNB)] with triamterene (TM) drug donors, which have many applications in industry, biology, and chemistry. The CT complexes of PA and 4-NP are formed by the association of electron-deficient and electron-rich moieties, held together by the weak force of attraction through a hydrogen bond. These molecules have been explored through the FTIR and Raman spectroscopic techniques. The speculated 1:1 or 1:2 structures of the complexes [(TM)(PA)], [(TM)(4-NP)₂], [(TM)(4-NAP)₂], and [(TM)(*m*-DNB)₂] determined by microanalytical and theoretical analyses shows that the interaction occurs through a $H_2N^+ - H \cdots O^- (O \cdots H)(O - H \cdots NH_2)$ bond or by $n - \pi^*$ regarding 4-NAP and *m*-DNB complexes. The thermogravimetric technique was utilized to determine the thermostability of the synthesized charge-transfer complexes by making comparisons to their constituents. The computational study has been carried out on the studied molecule, which has the most stable conformer using density functional theory (DFT). A comparative study of electronic and vibrational spectroscopy has been done with that of experimental results. The experimentally obtained structure was compared with an optimized structure for various parameters, such as bond length, bond angles, oscillator strength, dipole moment, and molecular electrostatic potential is predicted theoretically. The energy band gap from HOMO-to-LUMO was theoretically estimated using (B3LYP/6-311++G(d,p) level) from frontier molecular orbital energies, and the outcome data are employed to characterize the chemical structures of the synthesized complexes based on molecular properties.*

Keywords: triamterene, nitro organic acceptors, FTIR, charge-transfer, density functional theory, Raman spectroscopic.

СПЕКТРАЛЬНЫЙ АНАЛИЗ КОМПЛЕКСОВ С ПЕРЕНОСОМ ЗАРЯДА ПРЕПАРАТА ТРИАМТЕРЕНА С АКЦЕПТОРАМИ 2,4,6-ТРИНИТРОФЕНОЛОМ, 4-НИТРОФЕНОЛОМ, 4-НИТРОАЦЕТОФЕНОНОМ И *m*-ДИНИТРОБЕНЗОЛОМ В ТВЕРДОМ СОСТОЯНИИ

Abeer A. El-Habeeb

УДК 543.42;535.375.5

Научный колледж Университета принцессы Нуры Бинт Абдулрахман, Эр-Рияд 11671, Саудовская Аравия; e-mail: dr_abeer_2@hotmail.com

(Поступила 18 февраля 2020)

*Исследованы взаимодействия при переносе заряда между молекулами нитроорганических акцепторов 2,4,6-тринитрофенола (PA), 4-нитрофенола (4-NP), 4-нитроацетофенона (4-NAP) и *m*-динитробензола (*m*-DNB) с лекарственными донорами триамтерена (TM), которые широко применяются в промышленности, биологии и химии. Комплексы с переносом заряда PA и 4-NP образуются за счет объединения электронодефицитных и богатых электронами фрагментов, удерживаемых вме-*

** Full text is published in JAS V. 88, No. 2 (<http://springer.com/journal/10812>) and in electronic version of ZhPS V. 88, No. 2 (http://www.elibrary.ru/title_about.asp?id=7318; sales@elibrary.ru).

сте слабой силой притяжения через водородную связь. Эти молекулы исследованы с помощью ИК-Фурье-спектроскопии и комбинационного рассеяния света. Предполагаемые структуры 1:1 или 1:2 комплексов [(TM)(PA)], [(TM)(4-NP)₂], [(TM)(4-NAP)₂] и [(TM)(*m*-DNB)₂], определенные с помощью микроаналитического и теоретического анализа, показывают, что взаимодействие происходит через связь H₂N⁺-H...O(O---H)(OH---NH₂) или *n*-π* комплексов 4-NAP и *m*-DNB. Для определения термостабильности синтезированных комплексов с переносом заряда использован термогравиметрический метод. Методом теории функционала плотности исследована молекула, которая имеет наиболее стабильный конформер. Проведено сравнение экспериментальных результатов, полученных методами электронной и колебательной спектроскопии. Экспериментально полученная структура сравнивалась с оптимизированной структурой по таким параметрам, как длина связи, углы соединения, сила осциллятора, дипольный момент и электростатический потенциал молекулы, предсказанными теоретически. Ширина запрещенной зоны от HOMO до LUMO теоретически оценена с использованием уровня B3LYP/6-311++G(*d,p*). Полученные данные использованы для характеристики химических структур синтезированных комплексов на основе молекулярных свойств.

Ключевые слова: триамтерен, нитроорганические акцепторы, ИК-Фурье-спектроскопия, перенос заряда, теория функционала плотности, спектроскопия комбинационного рассеяния света.

Introduction. In recent decades, charge-transfer (CT) complexes have attracted growing interest because many products and contaminations have been detected in natural water, generating significant public concern. The idea of complexation has persuaded scientists to acquire basic, productive, and rapid strategies for the assurance and recognition of medications. Therefore, the science involved in CT interaction is of interest to researchers, drug specialists, and scientific experts. The detail of this type of interaction was first given by Benesi and Hildebrand [1]. These authors describe a novel band in the spectrum of charge-transfer complexes formed between benzene and iodine taking *n*-heptane as a solvent, which is absent either in the spectra of iodine or benzene.

The CT complex is considered useful as a photocatalyst [2] and in organic semiconductors [3, 4]. The phenomenon of the CT complex was first presented by Mullikan, who proposed a well-known theory [5] for the interaction that occurs between donor (electron-rich moiety) and acceptors (electron-deficient moiety). Later, contact of the CT complex was widely discussed by Foster [6], who showed that it occurs through the formation of a weak bond [7, 8]. It was also noted that the establishment of CTC generally begins with the change in color on mixing donor and acceptor, which absorbs radiation in the visible region [9–11].

Recently, the molecular pairs that form intermolecular CT complexes have been studied through density functional theory (DFT) [12–14]. Distribution of electronic charge among synthesized charge-transfer complexes with the assistance of DFT calculation enables us to directly describe the donor and acceptor. Therefore, in such cases, pre-assumption is not needed for charge distribution [15–17]. Moreover, TD-DFT has been performed to examine the FTIR spectra of four charge-transfer complexes, which affirmed the charge transfer transition between acceptor and donor moiety. To our knowledge, there is no theoretical examination of CT complex of triamterene (TM) with picric acid (PA), 3-dinitrobenzene (DNB), 2-nitrophenol (NP), and 2-nitroacetophenone (NAP). Hence, the present work targets completing such an investigation by DFT calculation on all four synthesized CT complexes.

Experimental details. Aldrich-Sigma Chemical Company supplied the pure triamterene drug, PA, 4-NP, 4-NAP, and *m*-DNB. IR spectra are registered by Bruker Spectrophotometer; Elemental analysis by Vario Elemental Analyzers CHN-932; Thermogravimetric analysis by Shimadzu TGA-50H analyzers; SEM Quanta by FEG 250, 20 kV; TEM by JEOL JEM-1200 EX II, 60–70 kV; XRD by X'Pert PRO PANalytical; and Raman laser by Bruker FT-Raman, laser 50 mW.

Charge-transfer solid complexes for the TM with PA, 4-NP, 4-NAP, and *m*-DNB were prepared by grinding of PA, 4-NP, 4-NAP, or *m*-DNB with TM with 1:1 molar ratio in a porcelain mortar with a few drops of CH₂Cl₂ solvent. The formed complexes were dark brown-to-olive green powder for TM-PA, TM-4-NP, TM-4-NAP, and TM-*m*-DNB complexes, respectively. The resulting solid chemical reactions were dried under vacuum then stored in clean capped vials.

Gaussian 09 Software [18, 19] has been used to perform the DFT/TD-DFT computations employing the Web MO interface [18, 19]. The calculations have been carried out on the charge-transfer complexes TM-PA, TM-4-NP, TM-*m*-DNB, and TM-4-NAP individually, whose 3D structure was drawn using ChemDraw Ultra 12.0. The molecular geometries of the complexes in an isolated gaseous phase were fully optimized under tight convergence criterion without any symmetry constraint by DFT at B3LYP-D3/6-31G(*d,p*) level

[20, 21]. Grimme's D3 dispersion correction was considered for weak interactions within complexes. Non-imaginary IR values obtained at optimized geometry using the same method corroborate the geometry at a minimum on potential energy surface. Some important IR bands were assigned high accuracy using animated modes by Gauss View 5 [22]. The assessment of uncertainties in data collected by the computational method has been done empirically (i.e., comparing the experimental and computational data directly to understand the level of precision anticipated). Also, using this theory, molecular electrostatic potential (MEP), we describe the frontier molecular orbitals (HOMO and LUMO), dipole moment, polarizability, chemical reactivity descriptors, and thermodynamic parameters (at 298.15 K) obtained using the B3LYP-D3/6-31G(*d,p*) method.

Result and discussion. *FTIR spectroscopy.* We performed a comparative study of four CT complexes of simulated IR (TM-PA, TM-4-NP, TM-*m*-DNB, and TM-4-NAP) with experimental data to detect different signals. The experimental FTIR spectra of four CT complexes are shown in Fig. 1. A couple of strong vibrational signals and animated modes of vibration are detected in the FTIR spectra of CT complexes, equivalent to the IR spectrum obtained by simulation (Figs. 2 and 3).

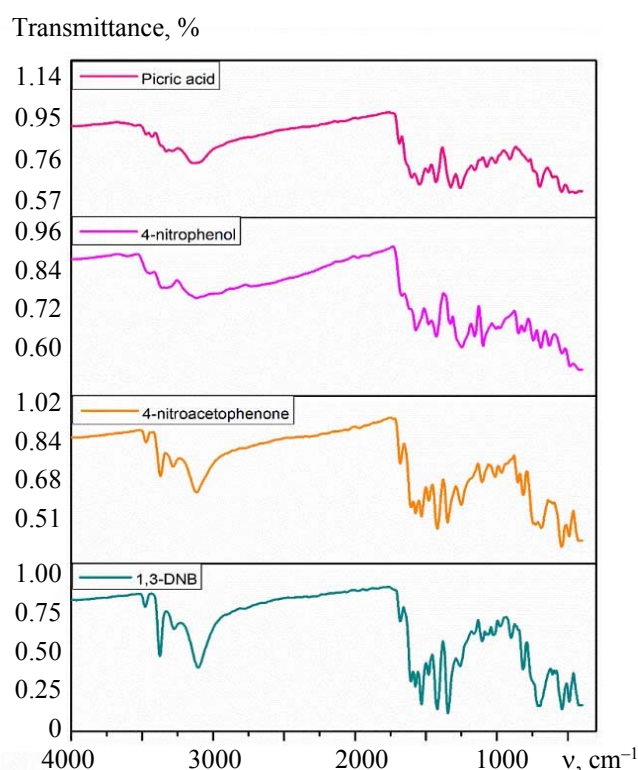


Fig. 1. FTIR spectra of TM with different acceptors such as PA, 4-NP, 4-NAP, and *m*-DNB.

In the TM with PA CT complex, in the experimental spectrum, the C-H aromatic stretching was detected at 3128.95 cm^{-1} , while a small shift in the wavenumber was seen in the spectrum, which is obtained by theoretical calculations. The transformation is also seen in the O-H band at 3329.8 cm^{-1} in the CT complexes. However, this has only a marginally higher wavenumber in the simulated spectrum. In this association, symmetric and asymmetric peaks of NH_2 were detected at 3429 and 3470 cm^{-1} , while it was noted from the literature that free amino groups in the pure TM were seen at 3371 and 3472 cm^{-1} , respectively. Subsequently, peaks of simulated amino groups were shifted to the higher wavenumber. Also, in the range of 1599 and 1428 cm^{-1} , peaks were assigned for the C-N and C=N bonds, which is comparable to the peaks obtained by theoretical calculations [23, 24].

Similarly, in CT complexes TM with 4-NP, the interaction occurs through O-H59----13NH₂ and O-H60----11NH₂. The peaks obtained for the aromatic C-H and O-H were observed at 3116.93 and 3329.61 cm^{-1} , whereas in the simulated spectrum, these peaks are shifted to the higher wavenumber. Furthermore, asymmetric and symmetric vibrational peaks are seen towards larger wavenumber than the experimental

data of the complex, which was pointed at 3439 and 3329 cm^{-1} , respectively. The C-N and C=N peaks were visible at 1570 and 1427 cm^{-1} , respectively, which is comparable to the data obtained by simulations.

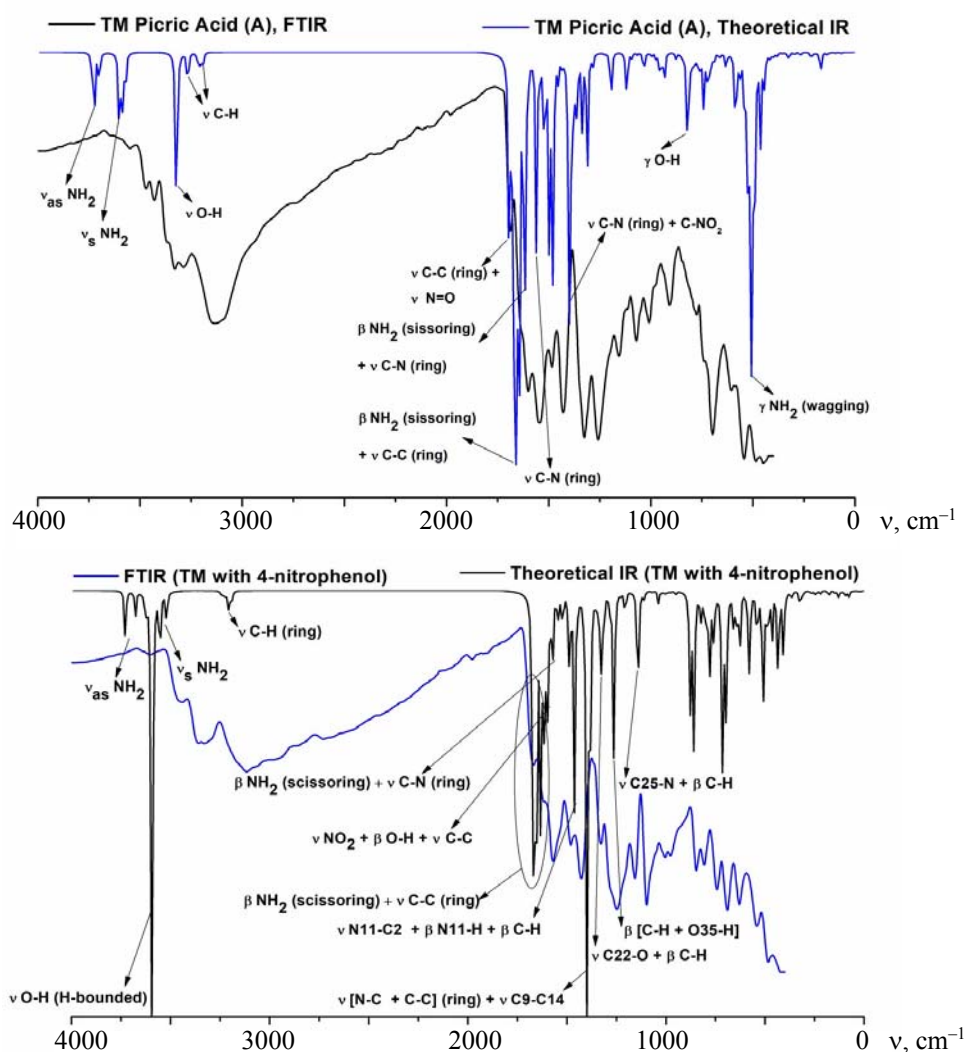


Fig. 2. Theoretical FTIR spectra of TM with PA and 4-NP.

It is observed from the spectrum of the CT complexes, which is complex formed between TM with 1,3-DNB, complexations occur by the interaction via $\text{O=N=O55} \cdots \text{H62-N-H}$ and $\text{O=N=O36} \cdots \text{H61-N-H}$. The aromatic C-H stretching was identified at 3104 cm^{-1} . A small shift in the wavenumber is found in the spectrum, which is acquired by the theoretical calculations. A couple of peaks were observed at 3477 and 3374 cm^{-1} , which is assigned for the asymmetric and symmetric amino groups of the CT complexes. We detected a slight difference in the case of the wavenumbers and intensities for the complex by comparison with the theoretical IR spectrum. The shift in C-N and C=N bond frequencies in the simulated spectrum of the CT complex were observed in which experimental peaks were marked at 1573 and 1418 cm^{-1} , respectively.

As explained above, the CT complex is formed by the interaction between TM and 4-NAP. An $\text{O=N=O37} \cdots \text{H24-C}$ and $\text{O=N=O49} \cdots \text{H54-N-H}$ bond has been developed because of the interaction between acceptor and donor. The aromatic C-H and O-H peaks were experimentally obtained within the region of $3115\text{--}3282 \text{ cm}^{-1}$, which is found slightly towards higher frequency in the simulated spectrum. Two peaks were seen at 3471 and 3371 cm^{-1} , which is appointed for the asymmetric and symmetric amino groups of the CT complex. There was little contrast in the wavenumbers and forces for the complex in examination with the theoretical IR spectrum. The frequency shifts to the larger number for C-N and C=N bonds in the simulated IR spectrum of the CT complex, which were seen at 1572 and 1418 cm^{-1} separately.

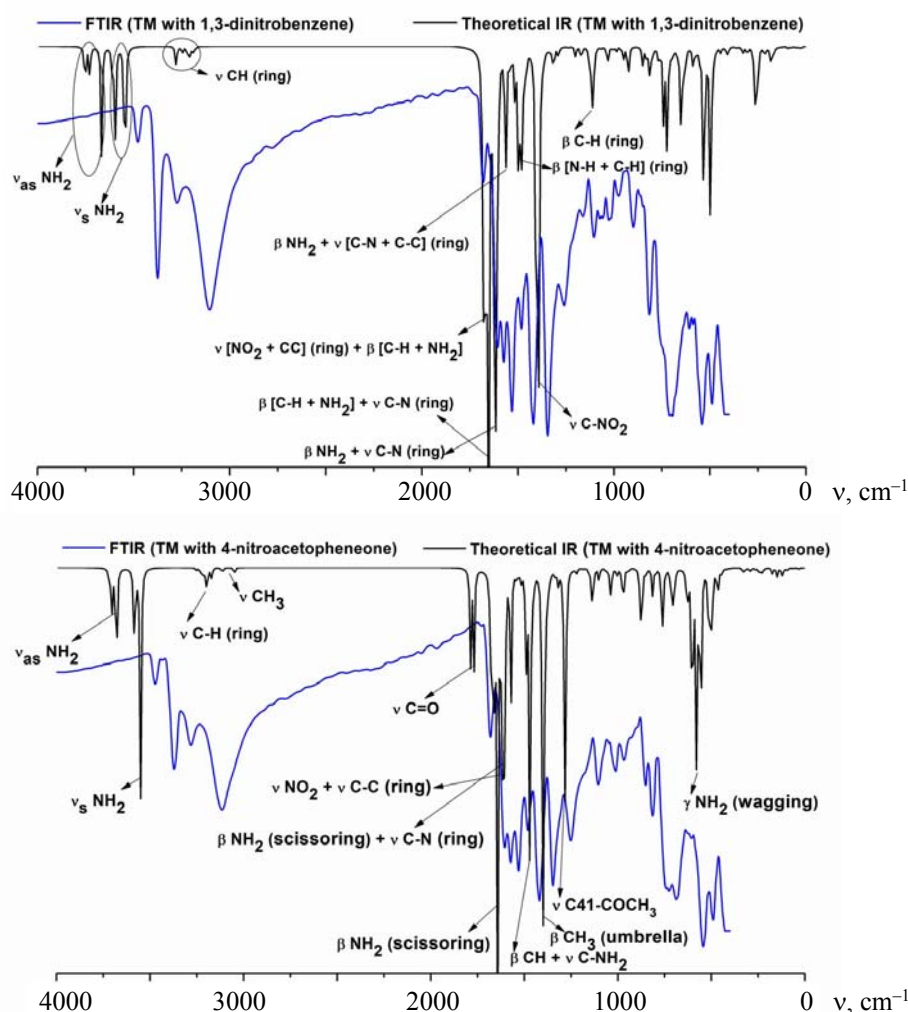


Fig. 3. Theoretical FTIR spectra of TM with 4-NAP and *m*-DNB.

Conductometry analysis. The conductivity of the CT complex of TM with different acceptors, such as PA, 4-NAP, 4-NP, and 1,3-DNB, was measured using dimethylformamide (DMF) as the solvent given in Table 1. The conductivity of the control was found to be 9.11 μs . It was noted that the conductivity increases, which may be due to the fact of different acceptors. The measured conductivities of the complexes [(TM)(DNB)], [(TM)(NAP)], [(TM)(NP)], and [(TM)(PA)] were 8.55, 9.33, 14.40, and 130.7 μs , respectively. It was concluded that the complex with higher conductivity is most stabilized in DMF solvent and that frequent complexation occurs.

TABLE 1. Conductance Data of TM-PA, TM-4-NP, TM-*m*-DNB, and TM-4-NAP Charge-Transfer Complexes

Sample	Different sample dissolved in Dimethylformamide (DMF)	
DMF	9.11 μs	Control
1	130.7 μs	TM-PA
2	14.40 μs	TM-4-NP
3	9.33 μs	TM-4-NAP
4	8.55 μs	TM-1,3-DNB

Powder XRD analysis. The powder XRD diffractograms of all four CT complexes are shown in Fig. 4. The crystalline nature of CT complexes was determined by the sharp, strong Bragg diffraction peak observed at different 2θ angles for complexes TM-1,3-DNB, TM-4-NAP, 4-NP, and TM-PA (i.e., 10.24°, 18.80°,

26.27°, and 43.38°, respectively). The XRD pattern reveals that the value of 2θ for TM-CT complexes increases. So, it was concluded that particle size also increases with the crystalline nature.

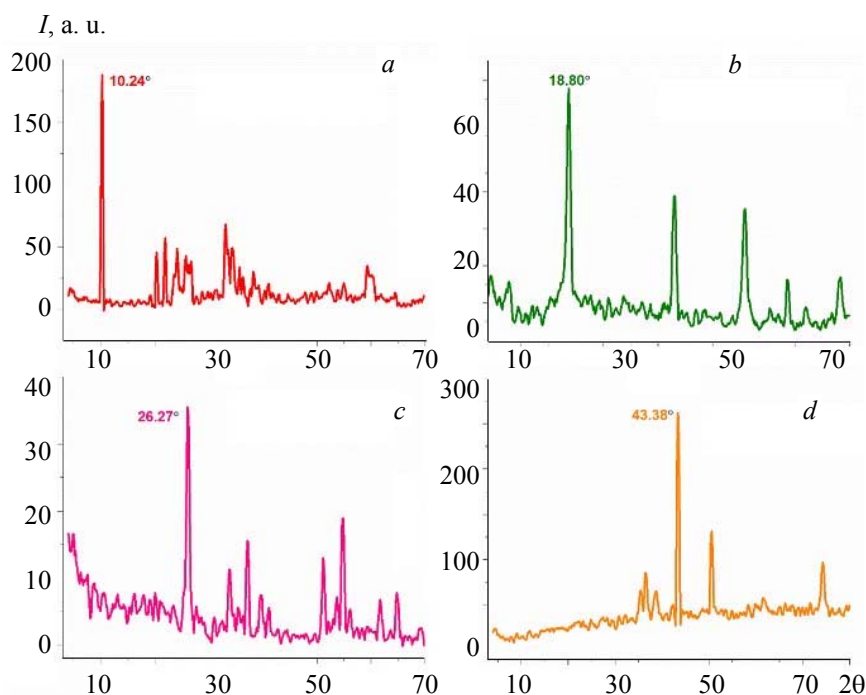


Fig. 4. XRD pattern of triamterene with different acceptors, (a) 1,3-DNB, (b) 4-NAP, (c) 4-NP, (d) PA.

SEM and TEM analysis. The SEM and TEM micrographs of the TM-PA, TM-4-NP, TM-*m*-DNB, and TM-4-NAP CT complexes were recorded to determine the size, shape, and uniformity of the synthesized complexes. It was seen from the SEM micrographs that all of the CT complexes have a different morphology showing the definite shape and homogeneous material. Figures 5 and 6 show the significant morphological changes observed between the CT complexes, which is due to the difference in the acceptor. Therefore, change in the acceptor affects the morphology of the CT complexes.

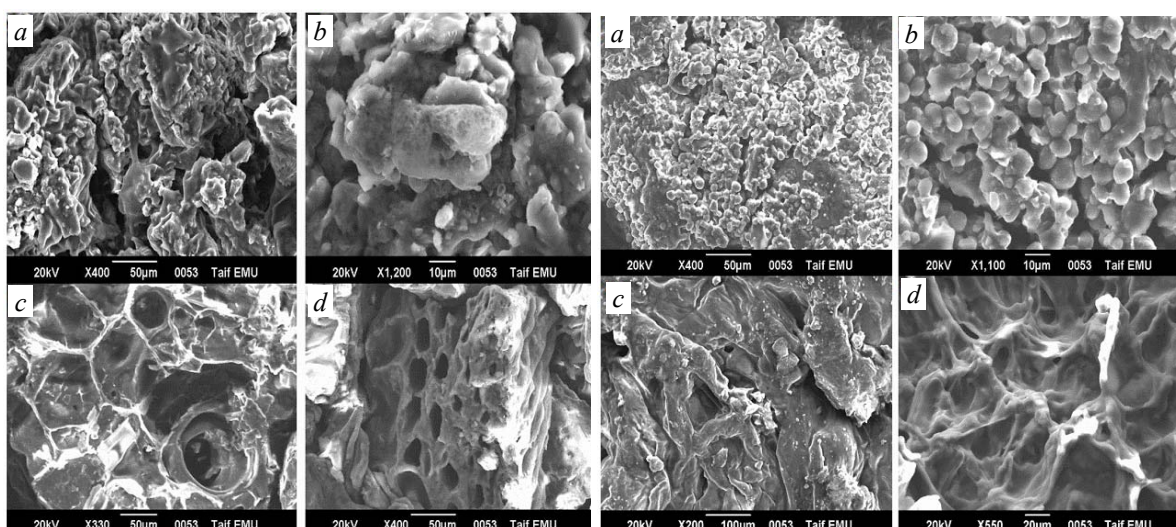


Fig. 5. SEM images triamterene with (a) and (b) *m*-DNB; (c) and (d) 4-NAP.

Fig. 6. SEM images of complex (a) and (b) TM-4-NP; (c) and (d) TM-PA.

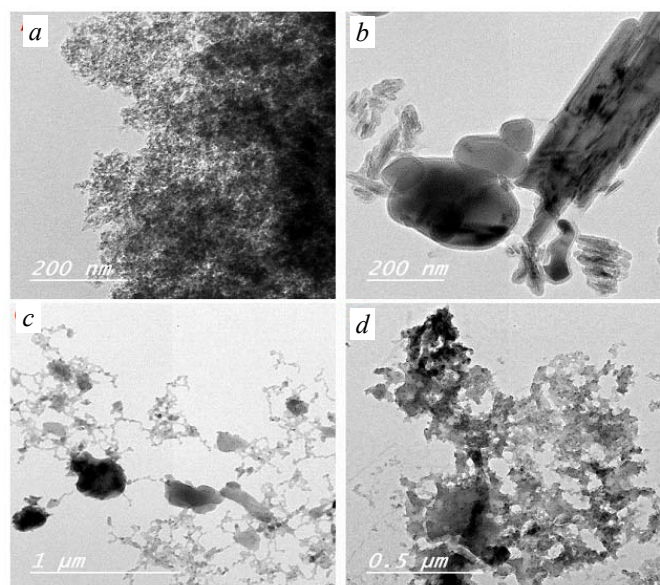


Fig. 7. TEM images of complex (a) TM-*m*-DNB; (b) TM-4-NAP; (c) TM-4-NP; (d) TM-PA.

Transmission electron microscopy (TEM) is shown in Fig. 7. It was seen from TEM images that all of the synthesized complexes are homogeneously dispersed, and particle agglomeration was observed. The size of the CT complexes TM-1,3-DNB, TM-4-NAP, 4-NP, and TM-PA are found to be 200, 200 nm, and 1, 0.5 μm , respectively.

Thermogravimetric analysis. Thermogravimetric analysis (TG) was done for the synthesized complexes of TM-CT within the range of 25–800°C. The weight loss of the samples was obtained as a function temperature from the TG curve shown in Fig. 8.

The curve for the CT complex of [(TM)(DNB)] shows a three-step degradation process. The first step degradation starts at 173.50°C with a weight loss of 3.71%, and the second degradation step corresponds to the weight loss of 3.32%, which is between 277.28 and 427.25°C. The third degradation step ranges between

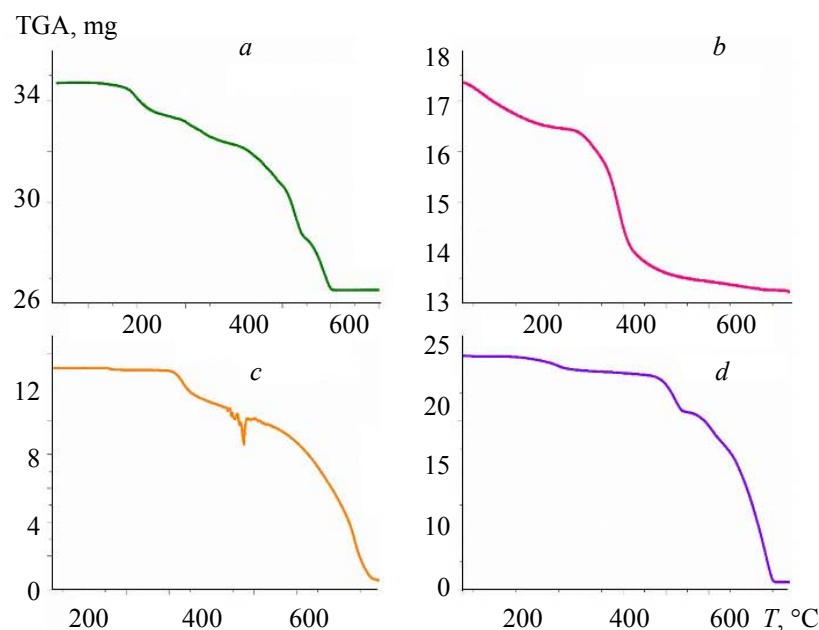


Fig. 8. TGA analysis of triamterene with (a) *m*-DNB; (b) 4-NAP; (c) 4-NP; (d) PA.

427.25 and 600.60°C, with a weight loss of 17.94%. The TG curve of [(TM)(NAP)] represents a two-step degradation in which the first step was between 25 and 298°C, and loss of mass was 5.2%. The second step starts after 298°C and continues until 800°C, with a mass loss of 19.06%. Similarly, the thermal decomposition of 4-NP with TM shows two degradation stages, with weight loss of 2.2 and 93% between temperatures 25 and 498.96°C and 498.96 and 796°C, respectively. Lastly, for the [(TM)(PA)] CT complex, the thermal curve shows two stages in the degradation of the CT complex in which the first step weight loss is 18% and the step two shows 72% decomposition between 25 and 565.65°C and 565.65 and 760.11°C respectively.

DFT based molecular properties. Some of the significant atomic parameters were estimated with the improvements of geometries for all the CT complexes. A recognizable transfer in the charge values in CT complex TM-PA is found for the atoms (O46, O44, H26, H38, and H23) associated with intermolecular hydrogen bonding through the formation of the complex and the relating energy minimized complex has appeared in Fig. 9. The plot of molecular electrostatic potential (MEP) for the CT complex (Fig. 10) is introduced to recognize the particular restricting destinations over the atom for electrophilic and nucleophilic assault. In all the CT complexes, various hues over the MEP surface demonstrate the idea of the electrostatic potential. The red, blue, and green areas inform about the negative, positive, and zero electrostatic potential, respectively. Negative and positive electrostatic possibilities are separately confined over the oxygen and hydrogen molecules. Individually, the areas with negative (red shaded) and positive (blue-hued) electrostatic possibilities might be the ideal destinations of electrophilic and nucleophilic assault.

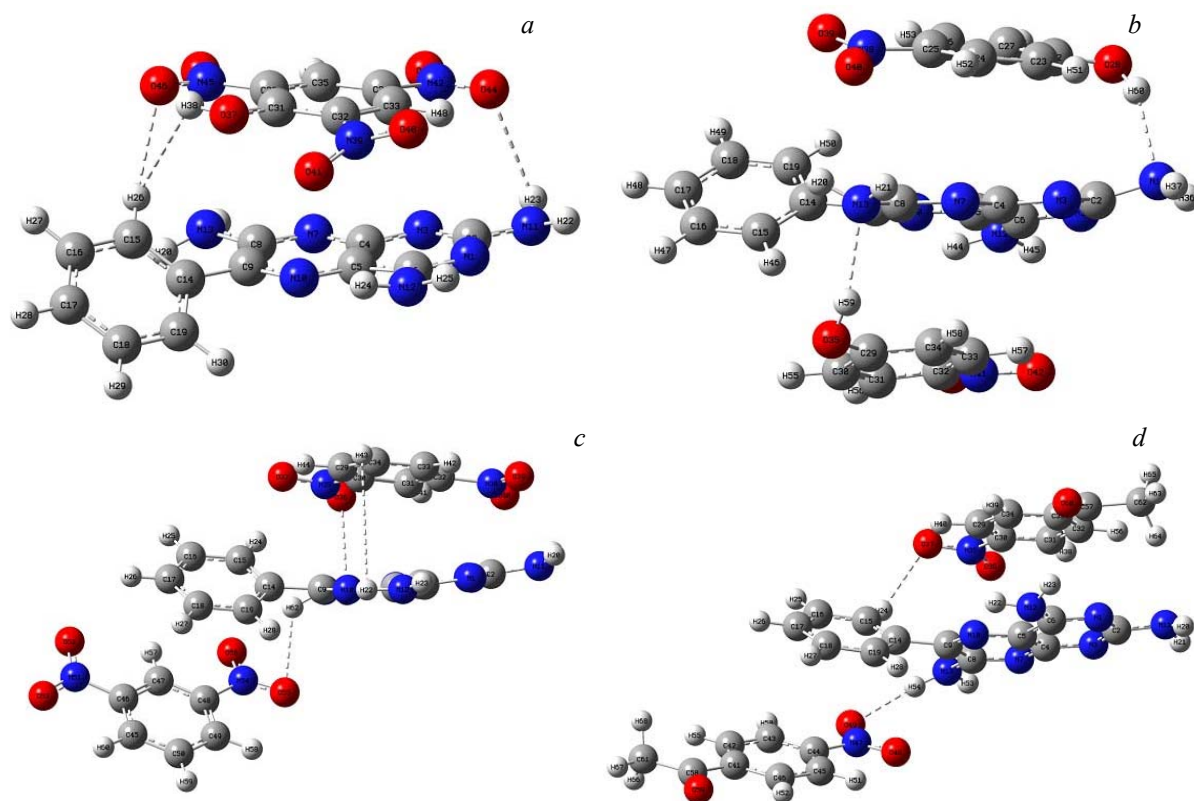


Fig. 9. Optimized structure of all the four CT complexes.

Charge delocalization inside the CT complex is explained by the frontier molecular orbitals for through highest occupied molecular orbital and lowest unoccupied molecular orbitals, and associated energies play an essential role in this explanation. Figures 11 and 12 show the spatial arrangements of the HOMO and LUMO, related energies, and HOMO–LUMO hole. It is discovered that the HOMO is confined over the triamterene moiety, while the LUMO is spread over the picric acid inside the CT complex TM-PA. Similarly, in the CT complexes TM-4-NP, TM-*m*-DNB, and TM-4-NAP, it is noted that the HOMO is obtained over the TM moiety while the LUMO is observed at 4-NP, 1,3-DNB, and 4-NAP, respectively. Table 2 details the different hypothetical sub-atomic parameters dependent on the enhanced structures for all four CT complexes in the gas phase (e.g., SCF energies, entropy, heat capacity, polarizabilities, thermodynamic parameters,

dipole moments, and HOMO–LUMO based CT complex reactivity descriptors for the CT complexes), and some interactions between TM and different acceptors for the optimized geometries are summarized in Table 3.

TABLE 2. Various Theoretical Molecular Parameters

Parameters	B3LYP-D3/6-31G(<i>d,p</i>)			
	TM-PA	TM-4-NP	TM- <i>m</i> -DNB	TM-4-NAP
SCF Energy, kcal/mol	-1109615.621	-1174263.374	-1336499.357	-1271434.504
Dipole Moment, Db	3.274590	2.138858	8.267666	3.711868
Polarizability	290.887732	318.957090	361.641121	376.872280
Thermal Energy (<i>E</i>), kcal/mol	236.051	304.821	303.944	349.098
Heat Capacity (<i>C_v</i>), cal/mol · K	112.681	130.447	140.606	147.827
Entropy (<i>S</i>), cal/mol · K	190.115	213.587	237.087	244.901
HOMO Energy (<i>E_H</i>) value, eV	-5.81	-5.98	-5.58	-5.46
LUMO Energy (<i>E_L</i>) value, eV	-3.57	-2.35	-3.39	-3.22
HOMO-LUMO gap, eV	2.24	3.63	2.19	2.24
Ionization Energy	5.81	5.98	5.58	5.46
Electron Affinity	3.57	2.35	3.39	3.22
Electronegativity	4.69	4.16	4.48	4.34
Chemical Potential	-4.69	-4.16	-4.48	-4.34
Hardness	1.12	1.82	1.09	1.12
Softness, eV ⁻¹	0.45	0.28	0.46	0.45
Electrophilicity	9.82	4.78	9.18	8.41

TABLE 3. Interactions Shown in Optimized Geometries

TM-PA	O=N=O46----H26-C	O-H-O44----H23-N-H	ring-ring
TM-4-NP	O-H59----13NH ₂	O-H60----11NH ₂	ring-ring
TM- <i>m</i> -DNB	O=N=O55----H62-N-H	O=N=O36----H61-N-H	ring-ring
TM-4-NAP	O=N=O49----H54-N-H	O=N=O37----H24-C	ring-ring

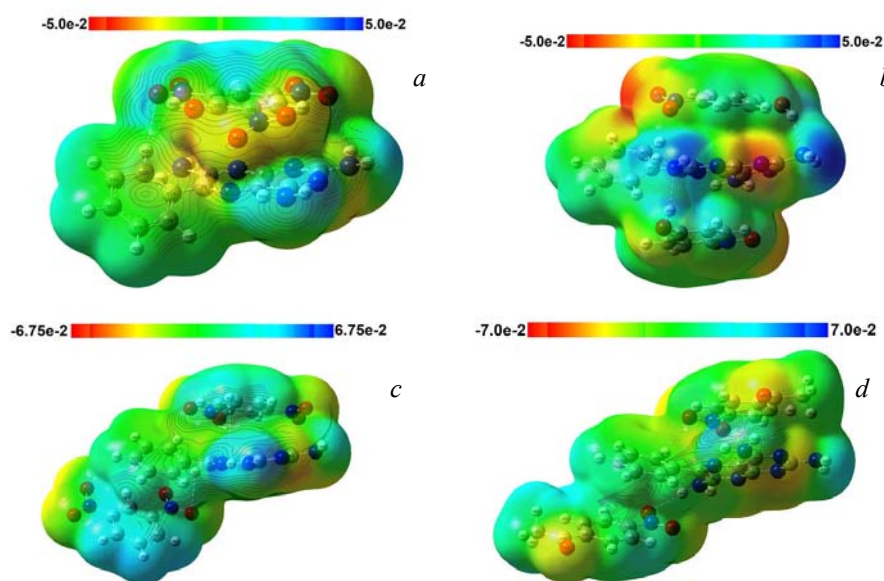


Fig. 10. MEP of TM with (a) 4-NP; (b) PA; (c) 1,3-DNB, and (d) 4-NAP.

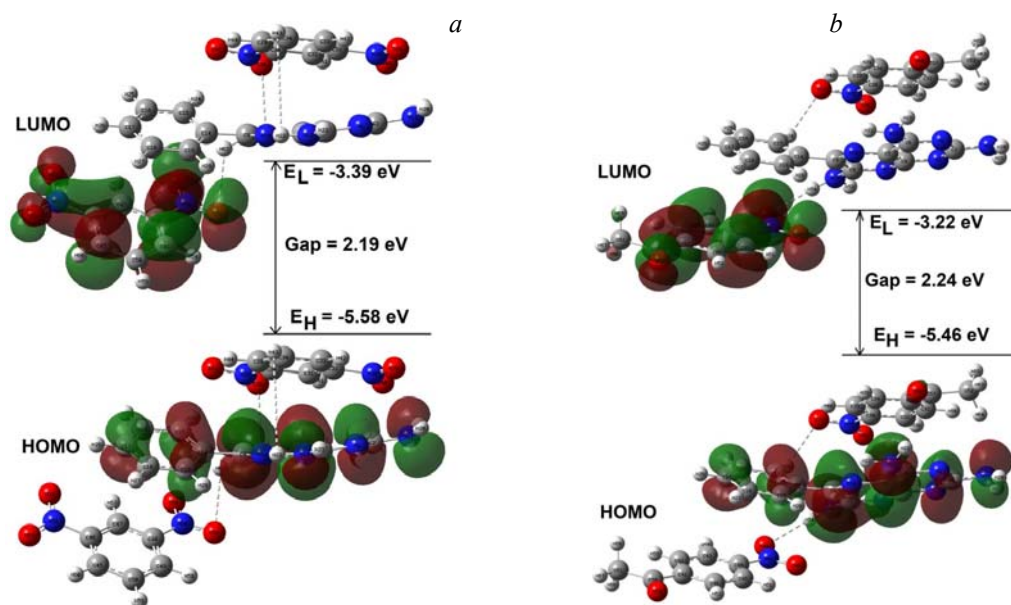


Fig. 11. Frontier molecular orbital of the CT complex (a) TM with 1,3-DNB; (b) TM with 4-NAP.

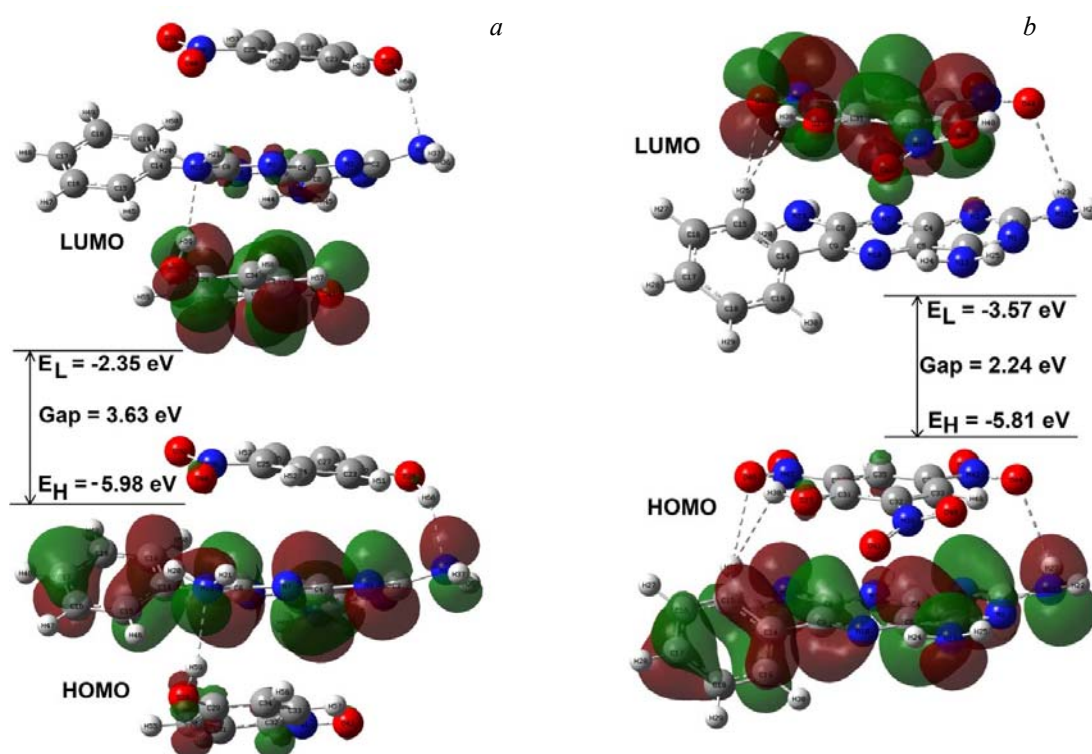
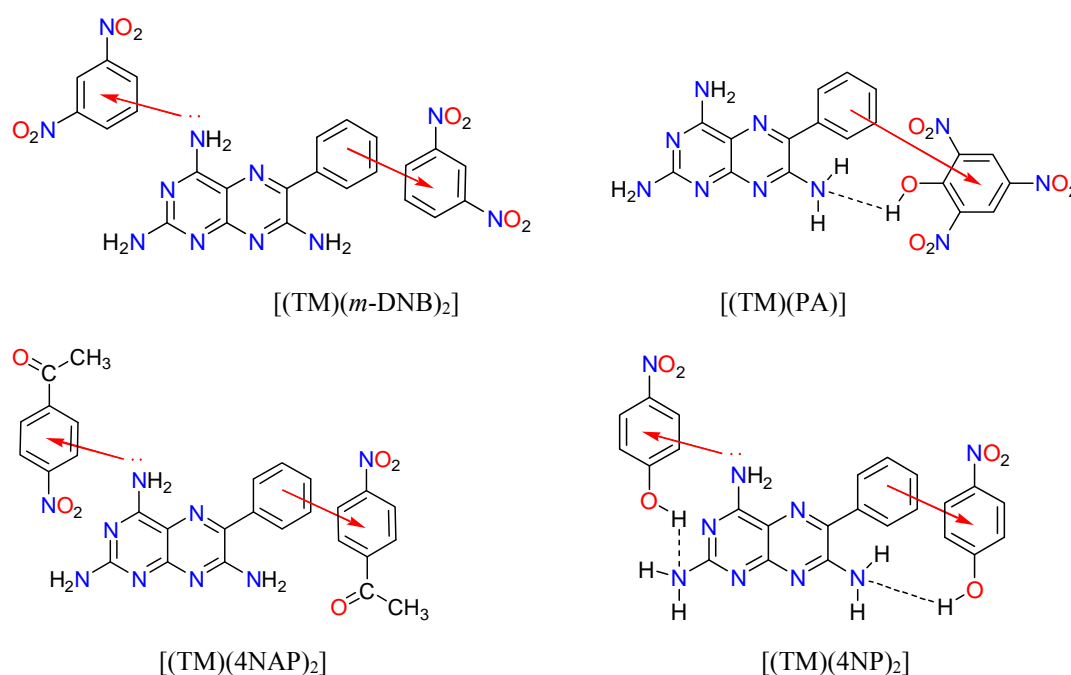


Fig. 12. Frontier molecular orbital of the CT complex (a) TM with 4-NP; (b) TM with PA.

Microanalytical analysis. Microanalytical data of the four CT complexes were listed in Table 4. The experimental of elemental analysis results confirmed that the TM-PA has a 1:1 molar ratio but the other CT complexes TM-4-NP, TM-*m*-DNB, and TM-4-NAP have 1:2 (donor:acceptor) stoichiometric ratio. Figure 13 is referred to the speculated structures of the CT complexes based on the spectroscopic, thermal and DFT analyses.

TABLE 4. Elemental Analysis of TM-PA, TM-4-NP, TM-*m*-DNB and TM-4-NAP Complexes

Formula	Molar mass	Found (Calculated), %		
		C	H	N
$[(TM)(m\text{-DNB})_2]$	589.48	48.21 (48.90)	3.51 (3.25)	26.87 (26.14)
$[(TM)(PA)]$	482.37	43.97 (44.82)	2.54 (2.93)	29.76 (29.04)
$[(TM)(4NAP)_2]$	583.55	57.93 (57.63)	5.01 (4.32)	21.70 (21.60)
$[(TM)(4NP)_2]$	531.48	54.31 (54.24)	4.09 (3.98)	24.01 (23.72)

Fig. 13. Speculated structures of $[(TM)(m\text{-DNB})_2]$, $[(TM)(PA)]$, $[(TM)(4NAP)_2]$, $[(TM)(4NP)_2]$, and CT complexes.

Conclusions. The theoretical and experimental IR spectra were compared and found to be in good agreement. This shows that the geometries of the complexes were correctly chosen. The theoretical FTIR frequencies were overestimated relative to the experimental frequency, mainly due to ignorance of the harmonicity in the calculations.

Acknowledgments. This research was funded by the Deanship of Scientific Research at Princess Nourah bint Abdulrahman University through the Fast-track Research Funding Program. Author also acknowledge the Chairman, Department of Chemistry, Aligarh Muslim University, Aligarh, for providing research facilities regarding the DFT calculations.

REFERENCES

1. H. Benesi, J. Hildebrand, *J. Am. Chem. Soc.*, **71**, No. 8, 2703 (1949).
2. R. Dabestani, K. J. Reszka, M. E. Sigman, *J. Photochem. Photobiol. A*, **117**, 223 (1998).
3. F. Vogtle, *Supramolecular Chemistry: An introduction*, Wiley, New York (1991).
4. A. Eychmuller, A. L. Rogach, *Pure Appl. Chem.*, **72**, 179 (2000).
5. R. S. Mulliken, *J. Am. Chem. Soc.*, **74**, 811 (1952).

6. R. Foster, *Organic Charge Transfer Complexes*, Academic Press, New York (1969).
7. R. S. Mulliken, *J. Am. Chem. Soc.*, **72**, 600 (1950).
8. R. S. Mulliken, W. B. Pearson, *Molecular Complexes*, Wiley Publishers, New York (1969).
9. M. M. A. Hamed, M. I. Abdel-hamid, M. R. Mahmoud, *Monatsh Chem.*, **129**, 4 (1998).
10. K. Alam, I. M. Khan, *Org. Electron.*, **63**, 7 (2018).
11. I. M. Khan, K. Alam, M. J. Alam, *New J. Chem.*, **43**, 9039 (2019).
12. A. Garcia, J. M. Elorzaand, J. M. Ugalde, *J. Mol. Struct. (Theochem)*, **501**, 207 (2000).
13. S. Fomine, L. Fomina, T. Ogawa, *J. Mol. Struct. (Theochem)*, **540**, 123 (2001).
14. S. Bhattacharya, M. Banerjee, A. K. Mukherjee, *Spectrochim. Acta A*, **57**, 2409 (2001).
15. A. Garcia, J.M. Elorza, J.M. Ugalde, *J. Phys. Chem. A*, **102**, 8974 (1998).
16. S. Reiling, M. Besnard, P. A. Bopp, *J. Phys. Chem. A*, **101**, 4409 (1997).
17. S. S. Chettu Ammal, S. P. Ananthavel, P. Venuvanalingam, M. S. Hegde, *J. Phys. Chem. A*, **102**, 532 (1998).
18. M. J. Frisch, et al., Gaussian 09, Revision D.01, Gaussian Inc, Wallingford CT, 2009.
19. J. R. Schmidt, W. F. Polik, WebMO Enterprise, version 18.1.001, WebMO LLC, Holland, MI, USA (2016), <https://www.webmo.net>, accessed July, 2018.
20. B. D. Becke, *Phys. Rev. A*, **38**, 3098 (1988).
21. C. Lee, W. Yang, R. G. Parr, *Phys. Rev. B*, **37**, 785 (1988).
22. R. Dennington, T. Keith, J. Millam, GaussView, Ver. 5, Semicem Inc, Shawnee Mission KS (2009).
23. M. J. Arias, J. M. Gines, J. R. Moyano, *Int. J. Pharm.*, **153**, 181 (1997).
24. A. P. Mukne, M. S. Nagarsenker, *AAPS PharmSciTech.*, **5**, 142 (2004).